


# Temperature and time dependent structure of the molten $Ni_{81}P_{19}$ alloy by neutron diffraction

U. Dahlborg[1], J.-G. Gasser[2], G. J. Cuello[3], S. Mehraban[4], N. Lavery[4], M. Calvo-Dahlborg[1,*]

[1]*GPM UMR6634-CNRS, University of Rouen Normandie, Campus Madrillet, BP12, 76801 Saint-Etienne-du-Rouvray cedex, France*

[2]*Université de Lorraine, Institut de Chimie, Physique, et Matériaux, 1 Bd Arago, 57078 Metz Cedex 3, France*

[3]*Institut Laue-Langevin, 71 Avenue des Martyrs, CS 20156, 38042 Grenoble Cedex 9, France*

[4] *Materials Research Centre, College of Engineering, Swansea University, Bay Campus, Fabian Way, Swansea SA1 8EN, UK*

*Corresponding author: M. Calvo-Dahlborg. Email: monique.calvo-dahlborg@univ-rouen.fr

Keywords: molten alloy, neutron diffraction, metastable state, time-dependent structure

**Abstract**

The temperature and time dependent structure of molten NiP alloy of eutectic composition has been studied by neutron diffraction. Ni particles were found to exist in the melt at temperatures at least up to about 150 degrees above liquidus. The amount varies reversibly as temperature increases but decays slowly with time. Remarkably, particles still exist even after that the melt has been kept more than 30 hours at different temperatures in the molten state. The static structure factor and the pair distribution function obtained at 1050$^{o}$C are presented.

## Introduction

It has been debated for a long time whether metals and alloys are homogeneous after melting or not at the atomic scale and this has been the subject of many theoretical and experimental studies. A variety of different experimental techniques have been used in order to find an answer to this question and results have been interpreted along different lines, one being that the structure of a molten alloy is inheriting much of the structure of the original ingot [1-5] while others are stressing the existence of strong short range order and atomic cluster formations (see for example [6]). An example of the theoretical approaches used to look at this problem are models for the structure of liquid alloys such as those developed in [7,8]. The possible existence of a liquid-liquid phase transition has been an issue for several investigations [9-15]. However, systematic experimental investigations in terms of composition, temperature and time dependencies of the physical properties of molten alloys have not been performed. Thus, in spite of all performed studies, a full understanding of the structure of a melt on a length scale going from some tens of a nanometer to several microns and its physical properties in terms of composition, temperature and time is still lacking.

In many investigations anomalies in measured property/temperature quantities (density, viscosity, surface tension, electrical resistivity, internal friction, etc.) of molten binary alloys are found during stepwise heating/cooling temperature cycles well above the liquidus temperature, while in other studies the quantities were found to vary in a regular way [16 and references therein]. Samples used for these studies are very often synthesized by mixing the elements by arc melting and an ingot for further studies is produced by casting. The ingot is afterwards re-melted several times in order to ensure that the sample to be studied is homogeneous with regard to its elemental composition and the measurements are performed in a heating/cooling sequence. However, the time and the temperature which are two very important parameters for the effect of the performed heat treatment of the ingot are very rarely mentioned. In other studies the melts to be studied have been produced in an induction furnace and the physical properties have been measured during cooling. These two fundamentally different ways to measure a specific physical property of a melt do not necessarily give the same result [16].

As mentioned above several explanations for the existence and non-existence of anomalies in measured physical properties have been given. In some cases the anomalies have been interpreted as indications of the existence of liquid-liquid phase transitions, while in others they have been found to be related not only to the thermal history of the melt but also of the ingot [1-5]. A possible presence and disruption of oxides during heating of the melt has also been suggested to influence the experimental results [17]. In other studies it has been suggested that the existence of atomic clusters in molten alloys is of thermodynamic origin and that the status of the melt corresponds to specific metastable temperature-dependent states [7, 18, 19]. Furthermore, it was shown that microheterogeneous states may exist as separate non-ergodic phases in molten binary alloys [20,21]. In all these cases a melt may be considered as a microstructural multi-phase system, a view that has been supported by results from investigations utilizing neutron and X-ray scattering techniques [20-25]. However, the influence of two very important parameters, temperature and time, on the existence of anomalies in the measured quantities has not been considered.

The influence of the melt status on the structure, the microstructure and the physical properties of vitrified $Ni_{81}P_{19}$ metallic glass ribbons but also several other glasses has been studied extensively [3, 4, 18, 22,23,26, 27, 29-32]. It was generally concluded from these studies that the nucleation and growth processes proceed along different routes depending on the thermal history of the melt and as a result, influences the microstructure of the solidified alloy. Studies of physical properties of the NiP system in solid phase as obtained from both experimental [33,34] and theoretical [36,36] investigations have also been performed. The relation between the structure of the melt and the structure of solidified alloy has also been discussed [23,27].

In this paper the time dependence of temperature changes on the structure of the eutectic NiP melt in a temperature region close to the liquidus is reported. The static structure factor and the pair distribution function are also presented.

**Theoretical background**

The measured intensity in a diffraction experiment on a disordered material is proportional to the total static structure factor $S(Q)$ that for a binary system in the Faber-Ziman formalism is given by [37]

$$S(Q) = \left\{ I_a^{coh}(Q) - \left[ < b^2 > - < b >^2 \right]^2 \right\} / < b >^2$$
$$= \sum_{\alpha} \sum_{\beta} c_\alpha c_\beta b_\alpha b_\beta S_{\alpha\beta}(Q) / < b >^2 \qquad (1)$$

$I_a^{coh}(Q)$ is the intensity per atom of coherently scattered neutrons and $c_i$ and $b_i$ are the concentration and scattering amplitude of atoms $\alpha$ and $\beta$, respectively. $<b>$ is equal to $c_\alpha b_\alpha + c_\beta b_\beta$ and $<b^2>$ to $c_\alpha b_\alpha^2 + c_\beta b_\beta^2$. $S_{\alpha\beta}(Q)$ is the partial structure factor, which describes the spatial correlations between α and β ions in the system. $Q$ is the wavevector transfer the neutron experiences in the scattering process and it is given by $Q=2k \sin(\Theta)$ where $k$ is the neutron wavevector and $2\Theta$ is the scattering angle. From the definition it follows that $S(Q)$ is equal to one at large $Q$. The scattering amplitudes for Ni and P are 10.3 and 5.13 fm and thus the relative weight factors in eq. (1) for the homogeneous eutectic NiP alloy are 0.80, 0.19 and 0.01, for $S_{NiNi}(Q)$, $S_{NiP}(Q)$ and $S_{PP}(Q)$, respectively.

**Experimental details**

The neutron diffraction experiments were performed on the D4 diffractometer at the Institute Laue-Langevin, Grenoble, France [38]. The wavelength of the incident neutrons was chosen to 0.703 Å. The corresponding $Q$ range was accordingly $0.4 < Q < 16.5$ Å$^{-1}$ and considered to be large enough to derive a reliable $g(r)$ from the measured $S(Q)$. The D4 instrument is equipped with 9 separate position sensitive detectors fixed relative to each other in a bank. Each detector is spanning a scattering angle range of 8 degrees. Thus, in order to scan the full angular range (i.e. from 1.5 to 140 degrees) the whole detector bank is rotated in a stepwise fashion. This means that the scattered intensity at a particular scattering angle ($Q$ value) is measured by several detectors but at different times according to the position of the detector bank. However, even if the intensity is not recorded simultaneously at every $Q$ it is possible to study the time dependence of particular features of the measured scattering curves.

The $N_{81}P_{19}$ sample ingot was made by melting pieces of metallic glass ribbons produced by melt spinning from very high chemical purity materials and reported in previous publications [23, 26, 27, 39]. The resulting ingot was introduced in a silica tube with an inner diameter of 15 mm and height about 70 mm. The silica tube was sealed under argon atmosphere and was

introduced in a standard ILL vanadium furnace, which allows temperatures up to about 1100°C to be reached. The lower edge of the neutron beam being set to a height of 18 mm was impinging on the silica tube 6 mm from its bottom. It is known that the NiP alloy is disintegrating because of the significant P vapor pressure developing at high temperatures for a P content larger than 40at.% [33]. Even with the tendency to disintegrate for smaller P contents, this experimental setup ensures that the measurements really are performed at the required melt composition. The temperature was measured by a pyrometer with a $\pm 2$°C accuracy. The time necessary in order to record diffraction patterns of relevant statistical accuracy for one position of the detector bank was about 20 minutes. In order to cover the entire $Q$ range patterns were recorded at 6 different detector bank positions.

The melting temperature for $N_{81}P_{19}$ published in the literature varies between 870°C to 891°C. In order to get more precise information and at the same time control the status of the amorphous ribbons, measurements with differential scanning calorimetry (DSC) were performed. The heating rate was chosen to 30K/min. Measured curves are shown in fig. 1 over two temperature regions, the first corresponding to the amorphous-to-crystalline transition and the second to the melting process. The curve in the first region has an identical shape to the one published in [27] on the same samples. The melting process, however, takes place at a somewhat lower temperature than the ones earlier published on alloys produced in different ways [33 and references therein].

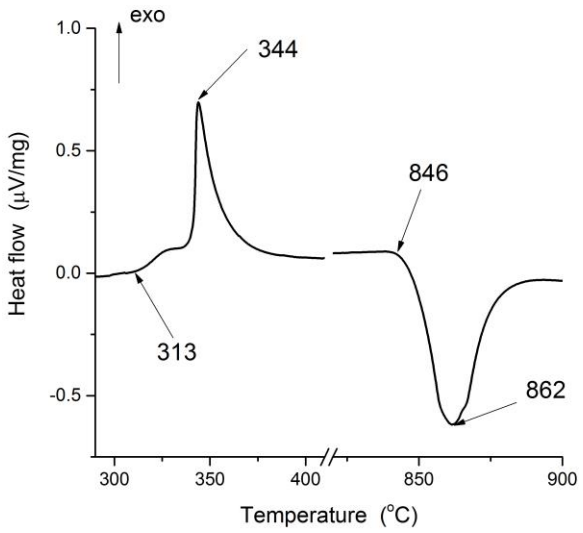

Fig. 1 Measured DSC curves in the temperature regions corresponding to the amorphous-to-crystalline transition (left) and the melting process (right). Relevant temperatures for the two processes are indicated.

The aim of the measurements was to determine the temperature dependence of the static structure factor $S(Q)$ but also to study the effect of a sudden temperature variation on its shape. For this purpose the time/temperature scheme shown in fig. 2 was adopted. The time for a temperature change was a few minutes.

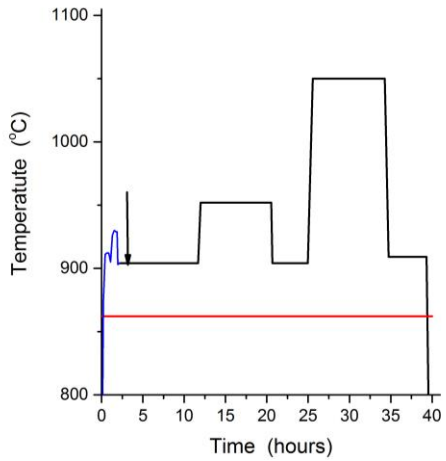


Fig. 2 The time-temperature variation scheme adopted for the neutron diffraction measurements. The horizontal line corresponds to the temperature of the melting peak shown in fig. 1. The arrow indicates the time the data recording started.

**Experimental results**

The NiP sample was kept at a temperature well above the melting point for more than three hours before the data recording started (see the arrow in fig. 2). The time-averaged static structure factor $S(Q)$ obtained during the 8.6 hours of measurement at a temperature of 904°C is shown in fig. 3. The $S(Q)$ curve has a shape characteristic of a molten system but some small superimposed peaks can also be seen. It can be concluded that in spite of the long holding time before the start of the measurement, well-defined crystalline inclusions are present in the melt. According to the phase diagram [33] the solidification of NiP of eutectic composition will result in the formation of Ni and $Ni_3P$ crystalline phases. As mentioned above the sample was made by melting metallic glass ribbons. The ribbons were highly likely to have an outer layer of oxides

but no sign of a presence of oxides within the neutron irradiated volume can be seen in the diffraction pattern shown in fig. 3. For comparison the positions of the diffraction peaks for fcc Ni and the most intense ones for tetragonal $Ni_3P$ taken from the Joint Committee on Powder Diffraction Standards (JCPDS) data sheet are shown at the bottom of fig. 3. It is obvious that the positions of the peaks observed in the measured curve correspond to the first five diffraction peaks in crystalline Ni and that no sign of crystalline $Ni_3P$ can be observed. The position of the Ni (111) diffraction peak coincides closely with the position of the main peak of $S(Q)$ and it can only be seen as a small asymmetry on its large Q side. On the other hand, the (200), (220), (311) and (222) peaks are clearly visible. In order to quantify the intensity of the peaks that were most easily separated, namely the (220) and (311) peaks, they were fitted with a sum of a Gaussian function and an interpolated background of parabolic shape. The widths of all peaks increased with increasing temperature but they were considered to be too close to the experimental resolution to allow for quantitative particle size estimation. However, it was nevertheless possible to conclude that the Ni particle size decreased with increasing temperature.

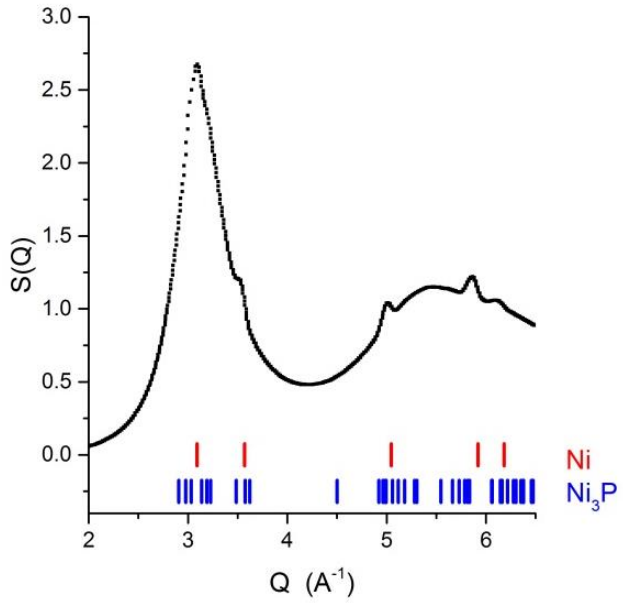


Fig. 3 Average static structure factor $S(Q)$ measured at 904°C during 8.6 hours starting at 3.1 hours after the start of the temperature loop shown in fig. 2. The vertical bars at the bottom of the figure indicate the positions of Ni and the most intense $Ni_3P$ diffraction peaks taken from the JCPDS crystallographic data sheets.

The specific features of the D4 diffractometer do not allow a continuous recording of a diffraction pattern but it is nevertheless possible to determine the time evolution of the melt structure. This is demonstrated in fig. 4 where the height of the main peak of $S(Q)$ measured during the entire 40 hour long measurements is shown. During this time the temperatures were changed according to the temperature variation scheme shown in fig. 2. It should be mentioned that the time to change from one sample temperature to the next was of the order of few minutes, thus considerably shorter than the time during which one separate pattern was recorded (about 20 minutes).

It can be seen in fig. 4 that the system responds very rapidly on every temperature change and that the intensity after this rapid change slowly decays during several hours. Every point corresponds to an average value of the peak height during the 20 minutes of recording. As was mentioned above the intensity of the main peak of $S(Q)$ is made up by two components, the most intense arising from the melt and a small contribution from the (111) peak of Ni. A first very intriguing feature in the intensity variation is that during the 8-hour measurement at 904$^{o}$C the peak height is decreasing from about 2.8 to about 2.6. This is even more remarkable, as before the recording started the melt was kept for about three hours at this temperature. The rate of intensity decrease seems to slowly flatten out with time. It can be anticipated that this is due to the decreasing contribution from the Ni (111) diffraction peak. The subsequent increase in temperature from 904 $^{o}$C to 952$^{o}$C results in a rapid first decrease in intensity after which the intensity slowly decreases during the following 8-hour measurement. The following temperature decrease to 904°C results in an instantaneous intensity increase which is followed by a slow decrease. Successive abrupt temperature changes result in similar intensity variations. It can be noted that the results obtained at 1050$^{o}$C gives the impression that the melt is homogeneous at this temperature.

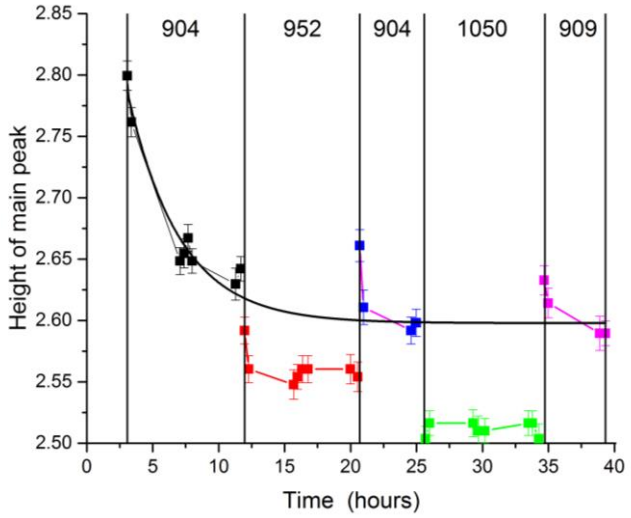


Fig. 4 The variation of the height of the main peak of the structure factor during the time-temperature variation scheme shown in fig. 2. The numbers at the top indicate the constant temperatures in ºC for the different time intervals. The curve is a result of a fit of eq. (1) to the data at the temperatures 904 and 909ºC as described in the text.

Another remarkable feature of the measured heights of the main peak of S(Q) presented in fig. 4 deserves to be stressed. Diffraction patterns were, as can be seen in fig. 2, measured close to 904ºC in three different time domains, 3 to 12, 21 to 26, and 34 to 39 hours after that the alloy was melted. It can be seen that the heights after the rapid variation following a temperature change seem to decay with temperature in a way as if the intermediate temperature changes have never occurred. In order to substantiate this notion the expression

$$I = A\, e^{-t/\tau} + B \qquad (1)$$

was fitted to the data. In the fit the intensities measured immediately after the temperature changes were omitted. The result of the fit is shown as the full curve in fig. 4. The relaxation time $\tau$ is found to be $4\pm1$ hours and B amounts to about $2.60\pm0.01$. In view of the rather large errors in the determination of these parameters we do not consider an application of this decay rate to be accurate enough in order to permit a reliable separation of the (111) Ni diffraction peak from the main diffraction peak and thus to determine a proper S(Q) at this temperature.

In order to study and to quantify the time/temperature dependent structure of the melt in more detail, the areas of the Ni (220) and (311) diffraction peaks are shown in fig. 5. The two

peaks exhibit very similar intensity variations both with regard to time and to temperature and, as could be observed in fig.5, the intensities of both decrease very slowly with time. It is furthermore obvious that the decay rate at 904$^{o}$C and at 909$^{o}$C seems to be independent from the fact that the melt, for a considerable length of time, has been kept a higher temperature. It can be concluded that Ni particles are present, although in varying amounts, in the melt even after that is has stayed 35 hours in the molten state. The creation of Ni particles due to the sudden temperature decrease is also clearly seen in fig. 5.

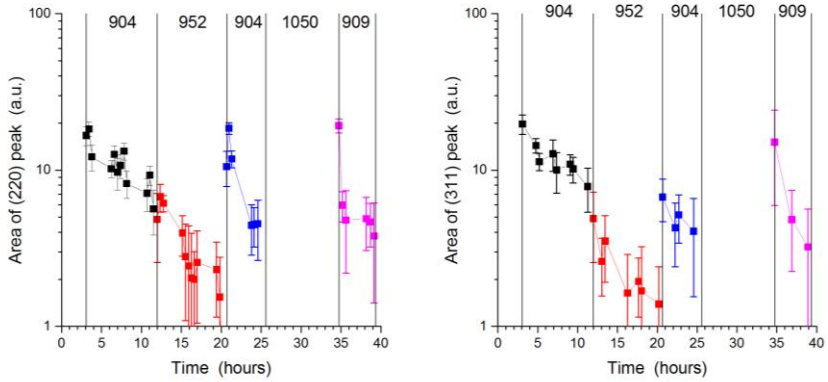


Fig. 5 The variation of the areas of (left) the (220) and (right) (311) diffraction peaks during the time-temperature scheme shown in fig. 2 The numbers at the top indicate the constant temperatures in $^{o}$C for the different time intervals.

The intensity variations of the Ni (220) and (311) diffraction peaks taking place during the first measurements at 904$^{o}$C and the second at 952$^{o}$C have been analyzed in more detail. The measured intensities were fitted by eq. (1) and the results are shown in fig. 6, while the obtained parameter values are given in table 1. The structural relaxation times $\tau$ are in all cases found to be about 4 hours for the (220) peak and somewhat shorter for the (311) peak. The values are very similar to the $\tau$ value found in the analysis of the main peak of S(Q), the result of which is shown in fig. 4. The fitted curves satisfactorily describe the experimental data but it has to be emphasized that the data may certainly be described also by other similar analytical expressions than the one in eq. (1) and that these might result in other values of derived relaxation times. For example, if a simple exponential decay of the data results is assumed, this results in $\tau$ values about twice as large as the ones shown in table 1. However, this does not obscure the fact, that as

can be seen in fig. 5 Ni particles that are large enough to be observed in a diffraction experiment exist in the melt during tens of hours.

| Temperature ($^{o}$C) | (220) diffraction peak | | (311) diffraction peak | |
|---|---|---|---|---|
| | τ (hours) | B | τ (hours) | B |
| 904 | 3.8±0.8 | 6±2 | 2.6±0.8 | 9±3 |
| 952 | 4.1±0.9 | 0.2±0.2 | 3.0±0.7 | 1.0±0.5 |

Table1. Parameters obtained from a least squares fit of eq. (1) to the data in fig. 6.

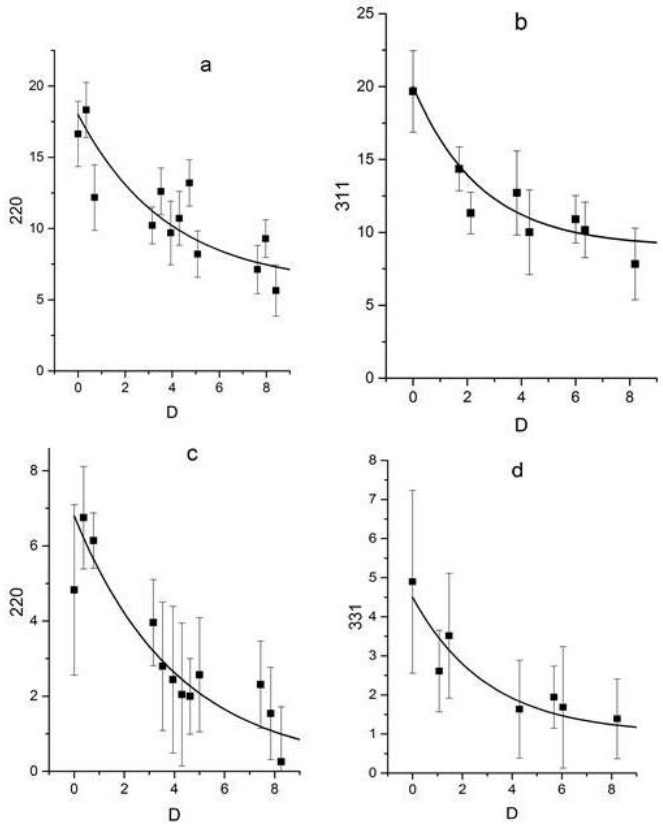


Fig. 6 Time variation of the Ni (220) and (311) diffraction peaks. a) the (220) peak during the first measurements at 904$^{o}$C and c) during the measurement at 952$^{o}$C. b) the (311) peak during the first measurements at 904$^{o}$C and d) during the measurement at 952$^{o}$C. The curves are obtained from a fit of eq. (1) to the experimental data.

The static structure factor $S(Q)$ and the corresponding pair distribution function $g(r)$ at 1050°C have been derived via an inverse Monte Carlo method assuming that the possible existence of Ni particles in the melt at this temperature can be neglected. The result is shown in fig. 7. Tries to derive S(Q) at lower temperatures by applying the temperature correction for the intensity of the Ni diffraction peaks have not given fully satisfactory results. The main peak of $S(Q)$ at 1050°C shown in fig. 7 is found at $Q = 3.11 Å^{-1}$, which is slightly smaller than the value given in [26, 39, 40], i.e. 3.127 $Å^{-1}$, for the metallic glass of the same composition. A small shoulder, however much less pronounced than in the metallic glass, can be seen on the large $Q$ side of the second peak indicating a non-uniform structure of the melt. This is also conjectured from small asymmetry at small r of the main peak of $g(r)$ in fig. 7b, which likely corresponds to Ni-P correlations as observed in the metallic glass [40]. The position of the main peak (2.47 Å) is slightly smaller than was observed for the metallic glass. As can be seen in fig. 7b the derived *g(r)* curve exhibits some small oscillations but, even if the statistical accuracy of the measured S(Q) (~0.1%) was excellent, it is not possible to conclude that these irregularities correspond to real structural effects, for example to the existence of small crystallization nuclei or to intermodulation of the partial pair distribution functions.

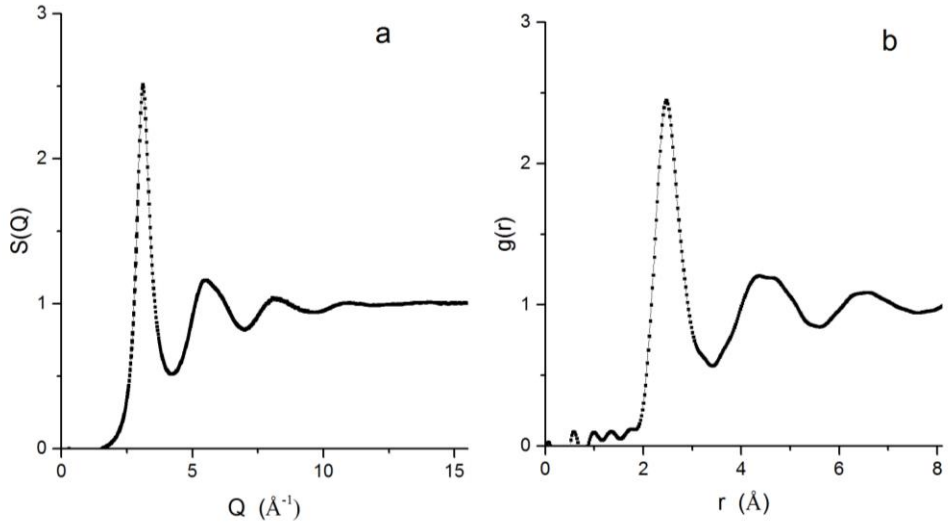


Fig. 7 (a) The structure factor $S(Q)$ and (b) the pair distribution function $g(r)$ for the $Ni_{81}P_{19}$ melt at 1050°C.

**Discussion**

The presence of anomalies in measurements of physical properties of molten alloys have been interpreted as indications that after melting the molten alloy is not homogeneous but consists of particles or clusters of atoms more or less tightly bound together and that are immersed in a eutectic molten matrix. The microheterogeneities are supposed to be inherited from the precursor solid alloy and they start to dissolve at a temperature $T_d$ considerably above liquidus. The melt does not reach a completely homogeneous state until heated to a temperature $T_b$ above well above $T_d$. [1-3]. It has furthermore been suggested that the existence of atomic clusters in molten alloys is of thermodynamic origin and that the status of the melt corresponds to specific metastable temperature-dependent states [18,19]. In both cases a melt may be considered as a microstructural two-phase system, a view that has been supported by results from investigations utilizing neutron and X-ray scattering techniques [18, 22-25]. Some of these results have been obtained indirectly, i.e. on metallic glass ribbons rapidly quenched from different states of the melt. The anomalies have also in some cases been interpreted as indications of the existence of a liquid-liquid phase transitions [10, 12].

Some few measurements of physical properties of molten alloys have been performed separating the two important parameters, temperature and time. However, recent studies have demonstrated the importance of such a separation. For example, measurements of the electrical resistivity in molten Pb-Sn alloys of two different compositions [43] have revealed that after an ultrasonic pulse the melt needs a time longer than two hours in order to recover. Furthermore, it was also shown that the viscosity in Al-rich melts of Al-Y during isothermal holding for several hours at temperatures more than 100 degrees above liquidus increases significantly before a subsequent exponential decay [44]. This increase in viscosity was explained by the temporal competition of two simultaneous effects, an Ostwald ripening effect in which large heterogeneities present in the melt after melting grow and a general slow dissolution of the heterogeneities resulting in a homogenization of the melt [45].

The most remarkable results presented above are that the life time of well-defined clusters in the eutectic NiP melt is of the order of 10 hours and that by temperature changes the microstructure of the melt can be controlled. However, structural reorganization times in

different kinds of liquids of the order hours and longer have earlier been reported [10 and refs therein]. For example, it was observed that 120 hours overheating at 700 degrees above the melting point was necessary to obtain a homogenous $Bi_{30}In_{70}$ alloy [17]. Furthermore, investigations by ultrasound techniques revealed that during a heating/cooling cycle up to temperature more than 900ºC above liquidus [41, 42] and lasting for more than 20 hours the attenuation coefficient in molten eutectic PdSi decreases considerably, not only during heating but also during the subsequent cooling. Another measurement has shown that a PbSn melt after an ultrasonic pulse needs several hours in order to return to its initial state [43]. A time of the same order of magnitude needed to reach a steady state in other molten alloys was found, for example, in the $Al_{95}Y_5$ alloy [44, 45]. Furthermore, similar behavior was observed in measurements of the kinematic viscosity, for example, in Al-rich Al-Fe melts [46], in FeB [47] as well as in BiZn melts [48]. The same phenomenon was also seen earlier in many ternary alloys [2, 49].

It is interesting to correlate the results presented above with the structure of Ni- and Fe-based metallic glass ribbons quenched after two different thermal treatments as presented in [26-29]. In one treatment the alloy was directly heated to 1110°C before quench and in a second one the alloy was heated to 1320°C, cooled to 1110°C and quenched. The holding time at every temperature was about 5 minutes. Neutron diffraction [26] and small angle neutron scattering measurements [23, 27] showed that none of the two ribbons was completely amorphous but contained crystalline inclusions, the ribbon quenched from a melt heated to 1320C though to a considerably smaller amount. Results, which can be interpreted according to the same lines, have been obtained for other molten alloys, for example for PdSi [41] and FeB [42]. Results for these alloys generally agree with the current ones indicating that crystallization nuclei are present in the melt at considerably higher temperatures than about 200 degrees above the melting temperature, although not detected in diffraction measurements because of their small size.

Together with results from earlier investigations using a variety of different experimental techniques the present work demonstrates that at least in some compositional ranges a molten alloy can be considered as a two-phase system and that, within a wide temperature range well after melting, it also contains clusters of atoms that might be inherited from the initial ingot [1-5 and references therein] but also correspond to metastable states of thermodynamic origin [16, 18,

19]. No obvious connection between the composition of these clusters and the crystalline stable phases found in the phase diagram seems to exist [16]. In this context, it should be mentioned that the presence of small amounts of oxides in many cases may have had a strong influence on a measured physical property and thus affected the results [17]. Accordingly, the preparation of the initial ingot is of outmost importance in this kind of measurements both in the liquid and in the solid state. Only at very high temperatures the microinhomogeneities as well as the macroheterogeneities existing in a certain temperature range above liquidus are dissolved and the alloy can be considered to be in a thermodynamically steady state.

## Conclusions

The structure of the molten NiP alloy of eutectic composition has been studied by neutron diffraction. Well-defined particles of Ni were found to exist in the melt at temperatures up to about 150 degrees above liquidus. The number of Ni particles decreases slowly with time but exist even after that the melt has been kept more than 30 hours in the molten state. A temperature change results in a reversible variation of the number of particles and suggests the existence of metastable melt/particle coexistence states.

The results clearly show the inadequacy of repeated melting/solidification schemes within a limited temperature range above liquidus in order to obtain a homogeneous melt for structural studies and measurements of physical properties.

## Acknowledgement

The authors are thankful to Institute Laue-Langevin, Grenoble, France for awarding beam time on the D4 diffractometer.

## References

[1] P.S. Popel, O.A. Chikova, V.M. Matveev, Metastable Colloidal States of Liquid Metallic Solutions, High Temp. Mater. Proc. 4 (1995) 219 - 233. https://doi.org/10.1515/HTMP.1995.14.4.219.

[2] V. Manov, P.S. Popel, E. Brook-Levinson, V. Molokanov, M. Calvo-Dahlborg, U. Dahlborg, V. Sidorov, L. Son, Yu. Tarakanov, Influence of the treatment of melt on the properties of amorphous materials: ribbons, bulks and glass coated microwires, Mater. Sci. Eng. A 304-306 (2001) 54-60. https://doi.org/10.1016/S0921-5093(00)01433-7.

[3] I.G. Brodova, P.S. Popel, G.I. Eskin, Liquid Metal Processing. Application to Aluminium Alloy Production, New York, Taylor and Francis, 2002.

[4] P.S. Popel, U. Dahlborg, M. Calvo-Dahlborg, Metastable microheterogeneity of melts in eutectic and monotectic systems and its influence on the properties of the solidified alloy, J. Non-Cryst. Solids 353 (2007) 3243-3253. https://doi.org/10.1016/j.jnoncrysol.2007.05.179.

[5] P.S. Popel, U. Dahlborg, M. Calvo-Dahlborg, On the existence of metastable microhetero-geneities in metallic melts, IOP Conf. Series: Mat. Sci. Eng. 192 (2017) 012012. https://doi.org/10.1088/1757-899X/192/1/012012.

[6] O.S. Roik, O.S. Muratov, O.M. Yakovenko, V.P. Kazimirov, N.V. Golovataya, V.E. Sokolskii, X-ray diffraction studies and Reverse Monte Carlo simulations of the liquid binary Fe-Si and Fe-Al alloys, J. Mol. Liq. 197 (2014) 215-222. https://doi.org/10.1016/j.molliq.2014.05.009.

[7] F. Sommer, Association model for the description of thermodynamic functions of liquid alloys, Pt. 1. Basic concepts, Z. Metallk. 73 (1982) 72-76.

[8] A.Z. Patashinskii, B.I. Shumilo, Theory of condensed matter based on the hypothesis of a local crystalline order, Zh. Eksp. Teor. Fiz. 89 (1985) 315-329. http://www.jetp.ac.ru/cgi-bin/dn/e_062_01_0177.pdf

[9] Y. Katayama, T. Mizutani, W. Utsumi, O. Shimomura, M. Yamakata, K.-I. Funakoshi, A first- order liquid-liquid phase transition in phosphorus, Nature 403 (2000) 170-173.. doi:10.1038/35003143.

[10] H. Tanaka, Bond orientational order in liquids: Towards a unified description of water-like anomalies, liquid-liquid transition, glass transition, and crystallization, Eur. Phys. J. E. 35 (2012) 113. https://doi.org/10.1140/epje/i2012-12113-y

[11] W. Xu, M.T. Sandor, Y. Yu, H.B. Ke, H.P. Zhang, M.Z. Li, W.H. Wang, L. Liu, Y. Wu, Evidence of liquid-liquid phase transition in glass-forming $La_{50}Al_{35}Ni_{15}$ melt above liquidus temperature, Nature Comm. 6:7696 (2015). doi:10.1038/ncomms8696

[12] F.Q. Zu, Temperature-induced liquid-liquid transition in metallic melts: A brief review on the new physical phenomenon, Metals 5 (2015) 395-417. http://dx.doi.org/10.3390/met5010395.

[13] S. Lan, M. Blodgett, K.F. Kelton, J.L. Ma, J. Fan, X.-L. Wang, Structural crossover in a supercooled metallic liquid and the link to a liquid-to-liquid phase transition, Appl. Phys. Lett. 108 (2016) 211907. https://doi.org/10.1063/1.4952724

[14] R.Z. Li, G. Sun, L.M. Xu, Anomalous properties and the liquid-liquid phase transition in gallium, J. Chem. Phys. 145 (2016) 054506. https://doi.org/10.1063/1.4959891

[15] Y.F. Lo, X.C. Wang, Z.D. Wu, W.Z. Zhou, H.W. Kui, Direct imaging of a first-order liquid-liquid phase transition in undercooled molten Pd-Ni-P alloys and its thermodynamic implications, J. Non-Cryst. Solids 472 (2017) 75-85. https://doi.org/10.1016/j.jnoncrysol.2017.07.020

[16] U. Dahlborg, M. Calvo-Dahlborg, D.G. Eskin, P.S. Popel, Chapter 8 in Thermal melt processing of metallic alloys, Springer, 2018, to be published

[17] K. Khalouk, M. Mayoufi, J.G. Gasser, Are there phase transitions in liquid metallic alloys?, Phil. Mag. 90 (2010) 2695-2709. http://dx.doi.org/10.1080/14786431003745310

[18] U. Dahlborg, M.J. Kramer, M. Besser, J.R. Morris, M. Calvo-Dahlborg, Structure of molten Al and eutectic Al-Si alloy studied by neutron diffraction, J. Non-Cryst. Solids 361 (2013) 63-69. https://doi.org/10.1016/j.jnoncrysol.2012.10.027.

[19] J.R. Morris, U. Dahlborg, M. Calvo-Dahlborg, Recent developments and outstanding challenges in theory and modeling of liquid metals, J. Non-Cryst. Solids 353 (2007) 3444-3453. https://doi.org/10.1016/j.jnoncrysol.2007.05.159.

[20] L. Son, Nonergodic correction to a binary mixture phase diagram, Physica A 449 (2016) 395-400. https://doi.org/10.1016/j.physa.2015.12.112

[21] L. Son, V. Sidorov, N. Katkov, Statistics and thermodynamics of Fe-Cu alloys at high temperatures, EPJ Web of Conferences 151 (2017) 05003. https://doi.org/10.1051/epjconf/201715105003.

[22] U. Dahlborg, M. Calvo-Dahlborg, P.S. Popel, V.E. Sidorov, Structure and properties of some glass-forming alloys, Eur. Phys. J. B 14 (2000) 639-648. https://doi.org/10.1007/s100510051073.

[23] M. Calvo-Dahlborg, U. Dahlborg, J.M. Ruppert, Influence of superheat before quench on the structure and stability of NiP metallic glasses studied by neutron scattering techniques, J. Non-Cryst. Solids 357 (2011) 798-808. http://dx.doi.org/10.1016/j.jnoncrysol.2010.12.003.

[24] M. Calvo-Dahlborg, P.S. Popel, M.J. Kramer, M. Besser, J.R. Morris, U. Dahlborg, Superheat- dependent microstructure of molten Al-Si alloys of different compositions studied by small angle neutron scattering, J. Alloys Compd. (2013) 9-22. https://doi.org/10.1016/j.jallcom.2012.09.086.

[25] F.G. Li, J. Zhang, Y.B. Dai, F.G. Bian, Y.F. Han, B.D. Sun, Study of the influence of $TiB_2$ particles on the melt structure of on the hypoeutectic Al-Cu alloy by small angle X-ray scattering, Mater. Chem. Phys. 143 (2014) 471-475. https://doi.org/10.1016/j.matchemphys.2013.10.027.

[26] U. Dahlborg, M. Calvo-Dahlborg, Influence of the production conditions on the structure and the microstructure of metallic glasses studied by neutron scattering, Mat. Sci. Eng. A283 (2000) 153-163. https://doi.org/10.1016/S0921-5093(00)00727-9.

[27] M. Calvo-Dahlborg, J.M. Ruppert, E.D. Tabachnikova, V.Z. Bengus, U. Dahlborg, F. Häussler, V.E. Sidorov, P.S. Popel, Influence of the heat treatment of the melt on the structure and mechanical behavior of metallic glass ribbons, J. Phys. IV France 11 (2001) 41-49. https://doi.org/10.1051/jp4:2001406

[28] V. Sidorov, P. Popel, M. Calvo-Dahlborg, U. Dahlborg, V. Manov, Heat treatments of iron-based melts before quenching, Mater. Sci. Eng. A 304-306 (2001) 480-486. https://doi.org/10.1016/S0921-5093(00)01499-4

[29] J. Miskuf, K. Csach, V. Ocelik, E.D. Tabachnikova, V.Z. Bengus, P.S. Popel, V.E. Sidorov, Influence of thermal treatment of Ni-P melt on structure of amorphous alloys, Czech. J. Phys. 54 (2004). D133-D136. 10.1007/s10582-004-0047-x.

[30] K.W. Chapman, P.J. Chupas, G.G. Long, L.A. Bendersky, L.E. Levine, F. Mompiou. J.K. Stalick, J.W. Cahn, An ordered metallic glass solid solution phase that grows from the melt like a crystal, Acta Mater 62 (2014) 58-68. https://doi.org/10.1016/j.actamat.2013.08.063

[31] A.A. Suslov, V.I. Lad'yanov, Effect of the liquid phase on the formation of orthorhombic boride during crystallization of $Fe_{82}B_{18}$ amorphous ribbons, Russian Metallurgy (Metally) 11 (2016) 1021-1026. https://doi.org/10.1134/S0036029516110148

[32] C. Liang, Z.-H. Chen, Z.-Y. Huang, F.-Q. Zu, Optimizing microstructures and mechanical properties of hypereutectic Al-18%Si alloy via manipulating its parent liquid state, Mater. Sci. Eng. A 690 (2017) 387-392. https://doi.org/10.1016/j.msea.2017.03.016

[33] C. Schmetterer, J. Vizdal, H. Ipser, A new investigation of the system Ni-P, Intermetallics 17 (2009) 826-834. https://doi.org/10.1016/j.intermet.2009.03.011.

[34] W.K. Luo, E. Ma, EXAFS measurements and reverse Monte Carlo modelling of atomic structure in amorphous Ni80P20 alloys, J. Non-Cryst. Solids 354 (2008) 945-955. https://doi.org/10.1016/j.jnoncrysol.2007.08.028.

[35] J.H. Shim, H.J. Chung, D. Nyung Lee, Calculation of phase equilibria and evaluation of glass-forming ability of Ni–P alloys, J. Alloys Compd. 282 (1999) 175-181. https://doi.org/10.1016/S0925-8388(98)00826-3.

[36] D.D. Zhao, L.C. Zhou, Y. Du, A.J. Wang Y.B. Peng, Y. Kong, C.S. Sha, Y.F. Ouyang, W.Q. Zhang, Structure, elastic and thermodynamic in the Ni-P system from first-principles calculations, CALPHAD 35 (2011) 284-291. https://doi.org/10.1016/j.calphad.2011.03.002.

[37] G.J. Cuello, Structure factor determination of amorphous materials by neutron diffraction, J. Phys.: Condens. Matter 20 (2008) 244109. https://doi.org/10.1088/0953-8984/20/24/244109

[38] H.E. Fischer, G.J. Cuello, P. Palleau, D. Feltin, A.C. Barnes, Y.S. Badyal, J.M. Simonson, D4c: A very high precision diffractometer for disordered materials, Appl. Phys. A 74 (2002) S160-S162 https://doi.org/10.1007/s003390101087

[39] M. Calvo-Dahlborg, F. Machizaud, S. Nhien, B. Vigneron, U. Dahlborg, Structural study of a phase transition in a NiP metallic glass, Mat. Sci. Eng. A 226-228 (1997) 197-203. https://doi.org/10.1016/S0921-5093(97)80037-8.

[40] P. Lamparter and S. Steeb, in Rapidly Quenched Metals, edited by S. Steeb and H. Warlimont (North-Holland, Amsterdam, 1985), Vol. 1, p. 459.

[41] G. Sivkov, D. Yagodin, S. Kofanov, O. Gornov, S. Volodin, V. Bykov, P. Popel, V. Sidorov, C. Bao, M. Calvo-Dahlborg, U. Dahlborg, D. Sordelet, Physical properties of the liquid Pd-18 at.% Si alloy, J. Non-Cryst. Solids 353 (2007) 3274- 3278.
https://doi.org/10.1016/j.jnoncrysol.2007.06.019.

[42] C.M. Bao, Etude sur la définition du terme « amorphe » par l'analyse comparative de rubans de $Pd_{82}Si_{18}$ en termes de production, structure, microstructure, qualité et propriétés mécaniques. Thèse de docteur de l'Institut National Polytechnique de Lorraine, 22/10/2007.
http://www.theses.fr/2007INPL068N#

[43] [15] X. Liu, J.F. Zhang, H.Y. Li, Q.C. Le, Z.Q. Zhang, W.Y. Hu, L. Bao, Electrical resistivity behaviors of liquid Pb-Sn binary alloy in the presence of ultrasonic field, Ultrasonics 55 (2015) 6-9. https://doi.org/10.1016/j.ultras.2014.07.008.

[44] V.I. Lad'yanov, S.G. Men'shikova, A.L. Bel'tyukov, B.B. Maslov, Influence of temperature and time of isothermal holding on the viscosity and crystallization processes of Al-Y melts close to a eutectic structure, Bull. Russ. Acad. Sci. Phys. 74 (2010) 1176-1178. https://doi.org/10.3103/S1062873810080423

[45] M.G. Vasin, S.G. Menshikova, M.D. Ivshin, Theoretical description of slow non-monotonic relaxation processes in Al-Y melts, Physica A 449 (2016) 64-73. https://doi.org/10.1016/j.physa.2015.12.085.

[46] A. L. Bel'tyukov, S. G. MenshikovaV. I. Lad'yanov, Viscosity of hypereutectic Aluminum-based Iron-alloyed melts, High Temperature 53 (2015) 491-496. https://doi.org/10.1134/S0018151X15030049

[47] A. L. Bel'tyukov, O.Yu. Goncharov, V. I. Lad'yanov, Russian J. Phys. Chem. 91 (2017) 1919-1924. https://doi.org/10.1134/S0036024417100065

[48] P. Jia, H.R. Geng, Y.J. Ding, M.Y. Li, M.X. Wang, S. Zhang, Liquid structure feature of Zn-Bi alloys with resistivity and viscosity methods, J. Mol. Liq. 214 (2016) 70-76. https://doi.org/10.1016/j.molliq.2015.12.004.

[49] V.I. Lad'yanov, A.L. Bel'tyukov, S.G. Men'shikova, V.V. Maslov, V.K. Nosenko, V.A. Mashira, Viscosity of glass-forming $Al_{86}Ni_8(La/Ce)_6$, $Al_{86}Ni_6Co_2Gd_4(Y,Tb)_2$ melts, Phys. Chem. Liq. 46 (2008) 71-77. http://dx.doi.org/10.1080/00319100701488508.